Supporting Information:

Mössbauer isomer shifts and effective contact densities obtained by the exact two-component (X2C) relativistic method and its local variants

Hong Zhu, Chun Gao, Michael Filatov, and Wenli Zou

November 3, 2020

Contents

1 The X2C Hamiltonian and its first-order derivatives

Starting from the four-component (4c) Dirac equation with embedded restricted kinetic balance, a matrix equation for the electronic (positive-energy) solutions was obtained by Dyall [J. Chem. Phys. 106, 9618, 1997],

$$\begin{pmatrix} \mathbf{V} & \mathbf{T} \\ \mathbf{T} & \mathbf{W} - \mathbf{T} \end{pmatrix} \begin{pmatrix} \mathbf{A}_+ \\ \mathbf{B}_+ \end{pmatrix} = \begin{pmatrix} \mathbf{S} & \mathbf{0} \\ \mathbf{0} & \frac{1}{2c^2}\mathbf{T} \end{pmatrix} \begin{pmatrix} \mathbf{A}_+ \\ \mathbf{B}_+ \end{pmatrix} \varepsilon_+ \, . \tag{S1}$$

By eliminating the small-component of the electronic wavefunction through

$$\mathbf{B}_+ = \mathbf{X}\mathbf{A}_+ \, , \tag{S2}$$

where $\mathbf{X}$ is the matrix representation of the relativistic transformation operator, Eq. (S1) can be simplified to

$$\tilde{\mathbf{L}}\mathbf{A}_+ = \tilde{\mathbf{S}}\mathbf{A}_+\varepsilon_+ \tag{S3}$$

with

$$\tilde{\mathbf{L}} = \mathbf{X}^\dagger\mathbf{T} + \mathbf{T}\mathbf{X} - \mathbf{X}^\dagger\left(\mathbf{T} - \mathbf{W}\right)\mathbf{X} + \mathbf{V} \, , \tag{S4}$$

$$\tilde{\mathbf{S}} = \mathbf{S} + \frac{1}{2c^2}\mathbf{X}^\dagger\mathbf{T}\mathbf{X} \, , \tag{S5}$$

where $\mathbf{S}$, $\mathbf{T}$, and $\mathbf{V}$ are the matrices of the overlap, kinetic energy and potential energy operators, $\mathbf{W}$ is the matrix of the relativistic operator $\frac{1}{4c^2}(\boldsymbol{\sigma}\cdot\mathbf{p})V(\mathbf{r})(\boldsymbol{\sigma}\cdot\mathbf{p})$. The relativistic transformation matrix $\mathbf{X}$ can be obtained either directly, e.g., by solving Eq. (S1) first and then inverting Eq. (S2) [J. Chem. Phys. 106, 9618, 1997; J. Chem. Phys. 126, 064102, 2007; J. Chem. Theory Comput. 8, 875, 2012], or by a number of iterative techniques [J. Chem. Phys. 106, 9618, 1997; Theor. Chem. Acc. 117, 333, 2007; Theor. Chem. Acc. 130, 633, 2011].

In the case of many-electron systems, the effect of relativity on the electron-electron repulsion integrals is typically ignored and the relativistically corrected one-electron Hamiltonian $\mathbf{H}^{\text{X2C}}$ is employed in connection with the non-relativistic many-electron formalism [J. Chem. Phys. 106, 9618, 1997; J. Comp. Chem. 23, 786, 2002; J. Chem. Phys. 131, 031104, 2009]. This requires renormalisation of the relativistic Hamiltonian in Eq. (S3) on the non-relativistic metric $\mathbf{S}$, which is carried out by

$$\mathbf{H}^{\text{X2C}} = \mathbf{R}^\dagger\tilde{\mathbf{L}}\mathbf{R} \, , \tag{S6}$$

with the renormalization matrix given by [J. Chem. Phys. 131, 031104, 2009]

$$\mathbf{R} = \left(\tilde{\mathbf{S}}^{-1}\mathbf{S}\right)^{1/2} = \mathbf{S}^{-1/2}\left(\mathbf{S}^{-1/2}\tilde{\mathbf{S}}\mathbf{S}^{-1/2}\right)^{-1/2}\mathbf{S}^{1/2} \, . \tag{S7}$$

Within the one-electron (1e) approximation, the Fock matrix is given by

$$\mathbf{F}^{\text{X2C}} = \mathbf{H}^{\text{X2C}} + \left(\mathscr{J} - \mathscr{K}\right) \tag{S8}$$

and the total electronic energy of the X2C Hartree-Fock (HF) or the X2C Kohn-Sham (KS) method is calculated as

$$E^{\text{X2C}} = tr\mathbf{P}\mathbf{H}^{\text{X2C}} + \frac{1}{2}tr\mathbf{P}\left(\mathscr{J} - \mathscr{K}\right) \, , \tag{S9}$$

$$\mathbf{P} = \mathbf{C}\mathbf{n}\mathbf{C}^\dagger \, , \tag{S10}$$

where $\mathscr{J}$ and $\mathscr{K}$ are the matrices of the Coulomb and the exchange operators, $\mathbf{P}$ is the density matrix, and $\mathbf{C}$ and $\mathbf{n}$ collect molecular orbital coefficients and occupation numbers, respectively. If contracted basis functions are used, $\mathbf{H}^{\text{X2C}}$ in Eq. (S9) has to be replaced by $\mathscr{H}^{\text{X2C}} = \mathscr{C}^\dagger\mathbf{H}^{\text{X2C}}\mathscr{C}$ where $\mathscr{C}$ collects the contraction coefficients.

Although the simplest 1e approximation to X2C was introduced above, the relativistic two-electron contributions can also be incorporated into X2C as well [Phys. Rep. 537, 59, 2014; J. Chem. Phys. 152, 180901, 2020].

Taking the derivative of the electronic energy in Eq. (S9) with respect to μ, where μ can be a nuclear coordinate, a component of the electric field, etc., one obtains

$$E_\mu^{\text{X2C}} = tr\mathbf{P}\mathbf{H}_\mu^{\text{X2C}} + tr\boldsymbol{\Omega}\mathbf{S}_\mu + \frac{1}{2}tr\mathbf{P}\left(\mathscr{J} - \mathscr{K}\right)_{\mu'} \, . \tag{S11}$$

Here, $\boldsymbol{\Omega}$ is the energy-weighted density matrix and the prime at μ' implies that only the two-electron integrals rather than the density matrix need to be differentiated. In Eq. (S11), only the first term on the right-hand side is different from the non-relativistic counterpart.

2 Effective contact density and contact density

For a series of selected neutral atoms, the (effective) contact densities have been calculated at the 4c-Dirac/PBE0 level of theory by DIRAC. The used basis set is Dyall's VTZ in the fully uncontracted form; for $Z_A \geq 52$ (Te) the basis functions are augmented by two tight s-functions and two tight p-functions (see Table S1). For $Z_A = 120$ (Ubn), the 37s34p14d7f primitive functions are taken from [Phys. Rev. A 2019, 99, 032509] and then augmented by 5d3f4g functions generated by the same formula.

Table S1: Augmented steep sp-functions for Dyall's VTZ basis set

Z_A	$\alpha_s^{(1)}$	$\alpha_s^{(2)}$	$\alpha_p^{(1)}$	$\alpha_p^{(2)}$
52 (Te)	1689533095.97318	326697399.67811	56152304.27179	18911298.82774
56 (Ba)	1636418314.74528	317058973.26979	77312232.25183	26840432.47170
70 (Yb)	1471705634.19654	283995415.70922	123968963.98426	47389003.17764
80 (Hg)	1387359534.19698	265526893.25905	150264660.70268	62603502.62282
88 (Ra)	1312197346.81460	251510427.78891	192319104.72396	97069967.65813
102 (No)	1232778360.37081	237305998.42427	193800567.35591	105887155.79496
112 (Cn)	1177648003.14108	227881680.34238	193370401.96021	111623241.44033

The (effective) contact densities and their ratios ($\rho_A^c/\rho_A^e = 1 + \varepsilon_A + \zeta_A$) are listed in Table S2, where ε_A is solely determined by Z_A at a given level of theory and ζ_A is much smaller than ε_A (see Table S4 below, for example), depending on physical and chemical environments, nuclear radii of isotopes, and so on.

Table S2: Contact densities, effective densities, and ratios of neutral atoms

Z_A	ρ_A^c (bohr^{-3})	ρ_A^e (bohr^{-3})	ratio	Z_A	ρ_A^c (bohr^{-3})	ρ_A^e (bohr^{-3})	ratio
1	0.3124	0.3124	1.0000	38	60703.2579	59460.6827	1.0209
4	35.4428	35.4426	1.0000	43	99842.6877	97191.3356	1.0273
8	315.2035	315.1973	1.0000	48	159067.3569	153802.7729	1.0342
12	1138.6792	1138.5415	1.0001	49	174273.7084	168271.3806	1.0357
14	1870.9854	1870.5615	1.0002	50	190491.0267	183654.9504	1.0372
16	2885.8513	2884.7476	1.0004	51	208359.7059	200585.8934	1.0388
18	4245.1813	4242.4403	1.0006	52	228555.2054	218346.4871	1.0468
19	5135.1895	5125.6759	1.0019	56	324035.9250	307392.2509	1.0541
20	6103.5466	6089.0573	1.0024	70	1043024.7202	961683.8690	1.0846
25	13044.6793	12975.6159	1.0053	80	2360932.3836	2125511.1163	1.1108
30	24872.9703	24644.6238	1.0093	88	4553585.5301	4014369.4689	1.1343
34	39447.7125	38915.4016	1.0137	102	14953926.4084	12651871.4347	1.1820
35	44055.1015	43415.6544	1.0147	112	36379325.3833	29792102.0191	1.2211
36	49031.2513	48262.0252	1.0159	120	76838820.9548	61071113.0179	1.2582
37	54695.9774	53651.0535	1.0195				

For neutral atoms (letting $\zeta_A = 0$ in this case), ε_A may be fitted as a function of Z_A

$$\varepsilon_A = \begin{cases} p_1(Z_A - 1)^2 + p_2(Z_A - 1)^4 & Z_A \in [1, 18] \\ p_1 Z_A + p_2 Z_A^2 & Z_A \in [19, 120] \end{cases} \tag{S12}$$

where the fitting parameters p_1 and p_2 have been listed in Table S3. The calculated and fitted ε_A values are plotted in Figure S2. Using Eq. (S12), effective densities may be estimated approximately by scaling contact densities.

Table S3: Fitting parameters in Eq. (S12)

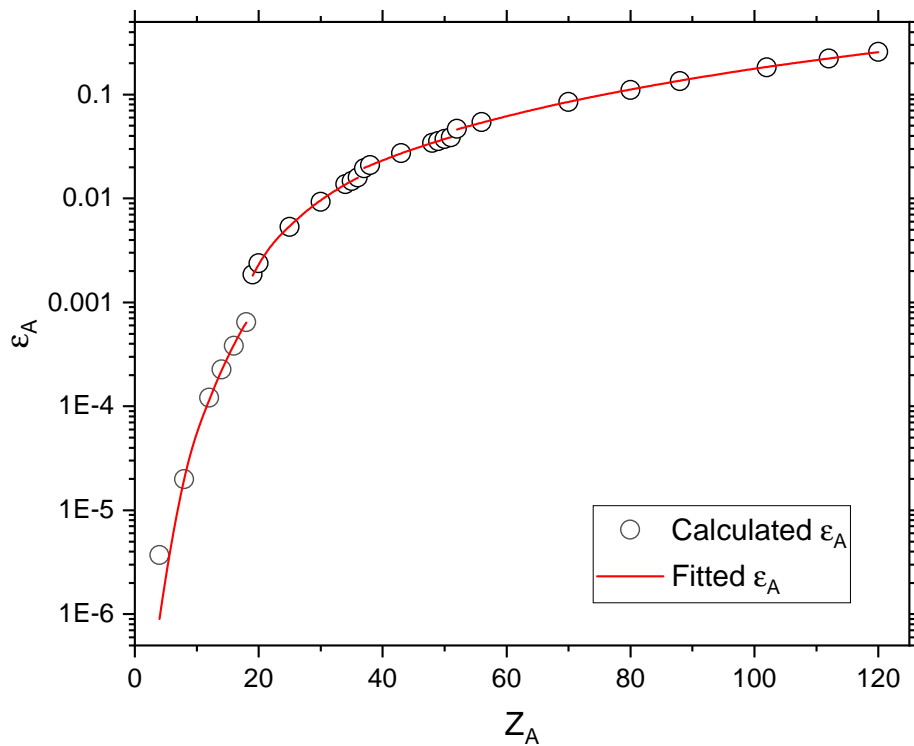| Z_A	p_1	p_2
1-18	3.50354×10^{-8}	7.54571×10^{-9}
19-36	-2.89331×10^{-4}	2.02493×10^{-5}
37-51	-7.77268×10^{-5}	1.64565×10^{-5}
52-120	-6.19084×10^{-5}	1.82206×10^{-5}

Figure S1: Calculated and fitted ε_A values relative to Z_A.

For a series of Cn ($Z_A = 112$) containing systems, the (effective) contact densities and ratios are calculated at the X2C/PBE0 level, where $\varepsilon_A \approx 0.2224$ for the neutral Cn atom and the ζ_A values are listed in Table S4.

Table S4: (Effective) contact densities and ζ_A values of Cn

	r_e (Å)	ρ_A^c (bohr^{-3})	ρ_A^e (bohr^{-3})	$10^8 \times \zeta_A$
Cn		36524922.21	29879227.13	0
CnF	2.108	36524880.87	29879193.55	-0.99
CnF$^+$	1.854	36524735.79	29879075.08	-1.87
CnF$_2$	1.926	36524549.15	29878922.85	-3.73
CnF$_4$	1.929	36524181.80	29878623.17	-7.11
CnO	1.863	36524967.49	29879264.55	-1.56
CnO$_2$	1.830	36524976.17	29879271.90	-2.58

3 One-particle density matrices of advanced ab initio methods

Table S5: One-particle (relaxed) density matrices of advanced ab
initio methods to generate natural orbitals

ab initio Method	Reference	Note
(SA-)MCSCF, (SA-)CASSCF	[a]	Eq. (7)
	[b]	Eq. (31)
(ic-)CASPT2	[c]	Appendix A
(ic-)MR-CISD, (ic-)MR-AQCC	[d]	Eqs. (70-72)
	[e]	see the discussion after Eq. (46)
CCSD	[f]	Eqs. (A20-A22)
	[g]	Eqs. (28,29,51)
CCSD(T)	[h]	Eqs. (8,9,15,16)
	[i]	Eqs. (7,8,27)
MP2, MP3, MP4, CCSDT	[j]	
RI-(SCS-)MP2	[k]	Eqs. (6-10)

[a] J. Chem. Phys. 150, 194106, 2019.
[b] J. Chem. Phys. 152, 074102, 2020.
[c] J. Chem. Phys. 119, 5044, 2003.
[d] J. Chem. Phys. 89, 5803, 1988.
[e] Mol. Phys. 100, 1647, 2002.
[f] J. Chem. Phys. 87, 5361, 1987.
[g] J. Chem. Phys. 95, 2623, 1991.
[h] J. Chem. Phys. 94, 442, 1991.
[i] Chem. Phys. Lett. 200, 1, 1992.
[j] J. Chem. Phys. 90, 1752, 1989.
[k] J. Comput. Chem. 28, 839, 2007.

4 Atomic density radial distributions of core orbitals

Most of the exchange-correlation (XC) functionals were optimized for the properties of valence electrons whereas their accuracies in core electrons (especially in heavy atoms) are not clear. As an example, the radon atom with 78 core electrons (Rn^{8+}) is calculated by the 22 most common XC functionals, including
APF (APFD without dispersion), B3LYP, B3PW91, BHandHLYP, BLYP, BP86, CAM-B3LYP, HCTH407, HSE06, M06, M06-2X, M06-L, M11, MN15, O3LYP, PBE0, SOGGA11X, tHCTH, tHCTHhyb, TPSSh, ωB97X (ωB97XD without dispersion), and X3LYP.

The scalar relativistic effects are taken into account by the sf-X2C Hamiltonian with the Gaussian-type finite nuclear model (FNM), and the basis set is Sapporo-DKH3-TZP-2012 (contracted with FNM) where the *s*-functions are uncontracted and augmented by two tight *s*-functions with the exponenets 7.195446e+08 and 1.444330e+08. The radical core density distributions ($\xi(R) = 4\pi R^2 \rho(R)$) of Rn^{8+} by different functionals are compared with the reference ones by sf-X2C/CCSD(T) natural orbitals without frozen cores, and the relative errors are plotted in Figure S4.

Figure S4 shows that the best three functionals are M06, HSE06, and PBE0 in both the nucleus region ($R \leq 0.01$ Å) and the core region, and a similar conclusion may be made for other rare gas ions. Among the three functionals, PBE0 has been widely supported by modern quantum chemistry programs.
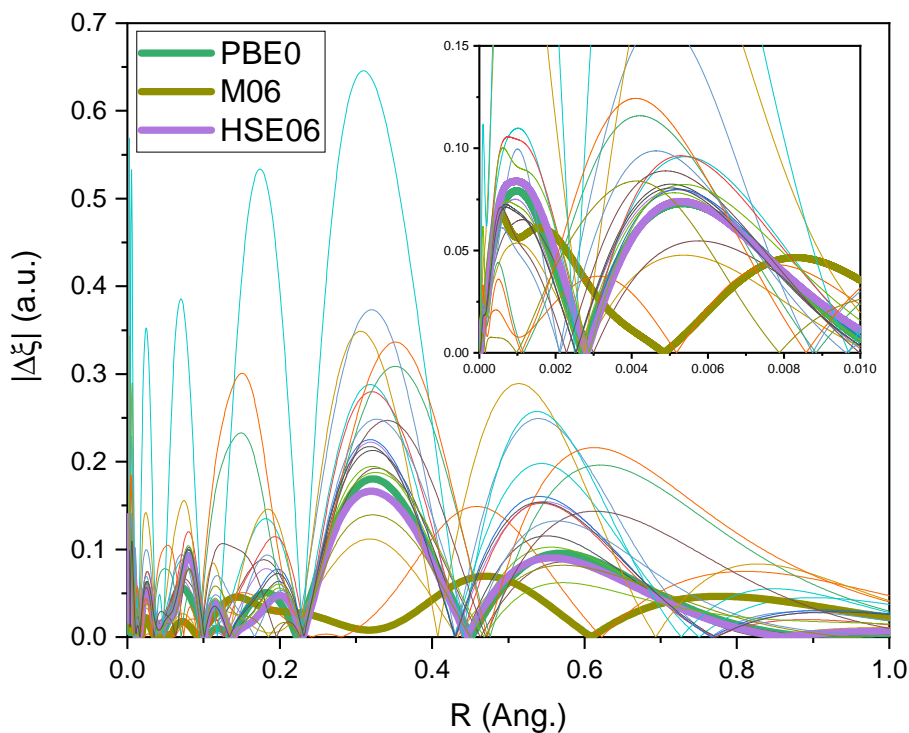

Figure S2: Error of density radial distributions of Rn^{8+} by different functionals.

5 Results for ^{57}Fe

As seen in Table S6, the effective densities of the iron atom may be decomposed into different occupied orbitals or spinors, which are calculated at the levels of non-relativistic HF, sf-X2C/HF, X2C/HF, and 4c-Dirac/HF with Dyall's uncontracted VTZ basis set.

The dominant contributions to effective densities come from the ns (n$s_{1/2}$) shells, but the np (n$p_{1/2}$) shells also contribute to the effective densities significantly due to the relativistic operator $\frac{1}{4c^2}(\boldsymbol{\sigma} \cdot \mathbf{p})V(\mathbf{r})(\boldsymbol{\sigma} \cdot \mathbf{p})$. However, the latter contributions are missing in non-relativistic calculations. As pointed by Knecht et. al. [Theor. Chem. Acc. 2011, 129, 631], other shells like $2p_{3/2}$ and $3d_{3/2}$ also make tiny contributions to effective densities (< 0.001 bohr^{-3} in the case of Fe).

Table S6: Effective densities (in bohr^{-3}) in different shells of Fe

Shell	non-rel.	sf-X2C	Shell	X2C	4c-Dirac
1s	10722.92	13393.64	1$s_{1/2}$	13393.61	13384.21
2s	986.27	1269.47	2$s_{1/2}$	1269.46	1268.83
2p	0.00	5.31	2$p_{1/2}$	5.82	5.80
			2$p_{3/2}$	0.00	0.00
3s	135.61	175.25	3$s_{1/2}$	175.26	175.11
3p	0.00	0.70	3$p_{1/2}$	0.77	0.77
			3$p_{3/2}$	0.00	0.00
4s	3.78	4.95	4$s_{1/2}$	4.95	4.95
3d	0.00	0.00	3$d_{3/2}$	0.00	0.00
			3$d_{5/2}$	0.00	0.00
total	11848.59	14849.34	total	14849.86	14839.67

The effective densities of Fe in some compounds by sf-X2C-AU without or with 1CA are collected in Table S7, in which the natural orbitals are computed at either sf-DKH2/RI-SCS-MP2 or sf-DKH2/ICE-SCF level of theory.

Table S7: Isomer shifts (in mm/s) and effective densities (in bohr^{-3}) of Fe in selected compounds

Species	2S+1	Expt. δ^{IS}	RI-SCS-MP2 orbitals		ICE-SCF orbitals		Coordinates
			sf-X2C-AU	1CA	sf-X2C-AU	1CA	
$FeCl_4^{2-}$	5	0.90	16455.73	16455.87	16454.57	16454.70	[a]
$Fe(CN)_6^{4-}$	1	-0.02	16460.57	16460.71	16459.88	16459.96	[a]
FeF_6^{4-}	5	1.34	16453.87	16453.96	16452.88	16452.96	[a]
$FeCl_4^{-}$	6	0.19	16459.12	16459.28	16458.50	16458.65	[a]
$Fe(CN)_6^{3-}$	2	-0.13	16460.40	16460.54	16459.96	16460.09	[a]
FeF_6^{3-}	6	0.48	16457.63	16457.75	16456.84	16456.93	[a]
$Fe(H_2O)_6^{3+}$	6	0.51	16457.93	16457.97	16457.00	16457.01	[a]
FeO_4^{2-}	3	-0.87	16463.42	16463.81	16464.70	16465.07	[a]
$Fe(CO)_5$	1	-0.18	16460.93	16461.19	16459.72	16460.05	[a]
$FeBr_6^{-}$	6	0.25	16459.31	16459.46	16458.80	16458.94	[b]
$Fe(H_2O)_5NO^{2+}$	4	0.76	16456.54	16456.64	16454.80	16454.91	[c]
$FeS_4C_8O_4^{2-}$	5	0.67	16457.28	16457.42	16455.66	16455.79	[c]

[a] Inorg. Chem. 48, 784, 2009 by TPSS.

[b] Inorg. Chim. Acta 337, 181, 2002.

[c] Inorg. Chem. 48, 9155, 2009.

6 Radical density distributions of Hg

At the sf-X2C/HF level, the radical density distributions of occupied shells of the Hg atom are plotted in Figure S3.
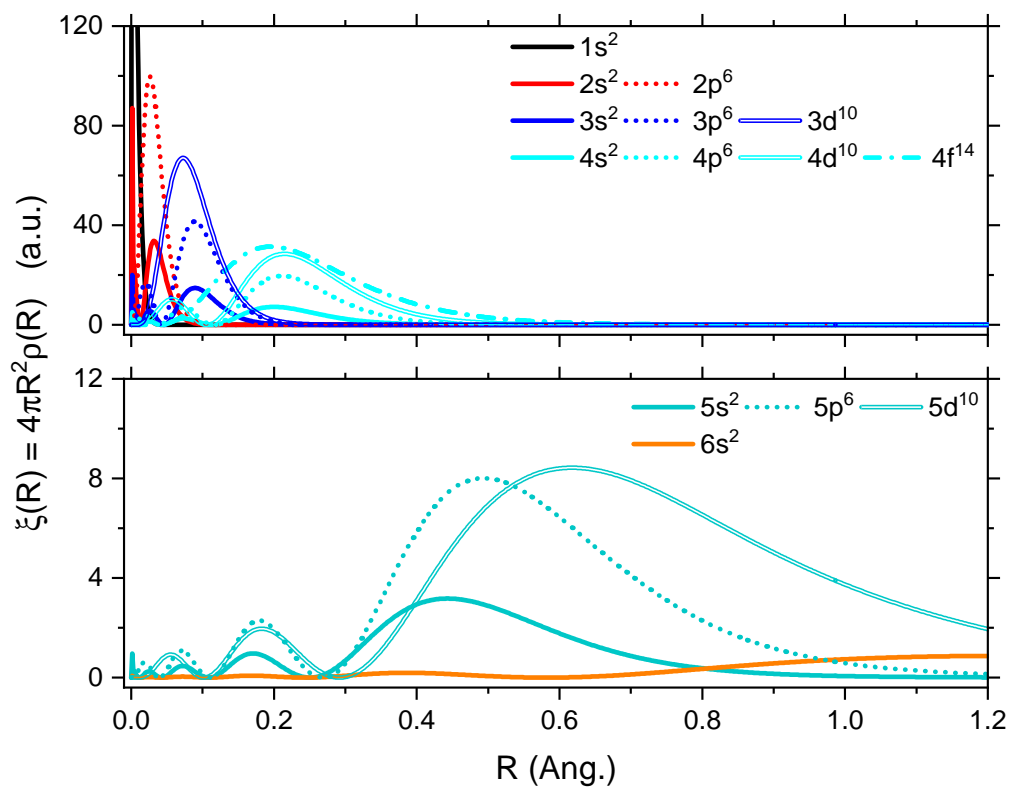

Figure S3: Radical density distributions of Hg.

7 About the RelED program

Molecular orbitals used in the RelED program may be calculated by the following relativistic Hamiltonians with FNM,

1. sf-X2C
   The sf-X2C Hamiltonian with FNM has been implemented in the quantum chemistry programs collected in Table S8, but some of them have not been supported or tested by the RelED program currently.

2. sf-BSS
   The BSS Hamiltonian (also called IOTC or IODKH) is closely related to X2C.

3. sf-DKHn
   The low-order Douglas-Kroll-Hess Hamiltonians (e.g. DKH2, DKH3, and DKH4) with FNM may work for the contact density of light atoms before $5d$ metals, but are not good choices for heavier atoms.

Molecular orbitals with point charge nuclear model (PNM) may also be possible for the calibration procedure, but this has not been fully tested.

Table S8: Quantum chemistry program list with FNM implemented

Program	Relativistic Hamiltonian	Data format
BAGEL	sf-DKH2	Molden; to be tested
BDF-G	sf-X2C, sf-BSS, sf-DKHn	Molden
CFour [a]	sf-X2C	Molden
Cologne	sf-X2C	Molden, Fchk [b,c]
	X2C	Fchk [c]
Columbus [d]	sf-X2C, sf-BSS, sf-DKHn	Molden; to be tested
Dalton	sf-DKH2	Molden; to be tested
Gaussian	sf-DKH2	Fchk [b,c]
	DKH4	Fchk [c]
(Open)Molcas	sf-X2C, sf-BSS, sf-DKHn	Molden; to be tested
Molpro [e]	sf-X2C, sf-DKHn	Molden
MRCC [f]	sf-X2C	Molden
NWChem [g]	sf-DKH2, sf-DKH3	Molden; to be tested
ORCA	sf-DKH2	Molden
PySCF	sf-X2C	Molden; to be tested

[a] Since CFour 2.1.

[b] Multiwfn is needed to get a Molden file.

[c] An interface to the Fchk file will be available soon in RelED.

[d] Through the interface to (Open)Molcas.

[e] Since Molpro 2019.

[f] Through the interface to CFour.

[g] Since NWChem 7.0.